Control Barrier Functionals for Safety-Critical Control of Registration Accuracy in Roll-to-Roll Printing Systems

Zhiyi Chen, Gábor Orosz, *Senior Member, IEEE*, and Jun Ni

***Abstract*—A control framework that optimizes registration accuracy while ensuring safety in roll-to-roll processes is presented. A primary controller using a modified algebraic Riccati equation is designed to reduce registration errors. This is complemented by a safety-critical controller based on a control barrier functional to maintain tension within safe limits. Our method is supported by numerical simulations, offering great potential to enhance existing industrial controllers.**

***Index Terms*—Control barrier functional, manufacturing system, roll-to-roll registration, safety-critical control.**

I. Introduction

THE MANUFACTURING of thin-film devices plays a vital role in various industries, ranging from electronics to renewable energy. As the demand for high-volume production increases, there is a growing interest in adopting roll-to-roll (R2R) methods due to their potential for high-speed and continuous manufacturing. While R2R processes excel in scalability and efficiency, they yield low registration accuracy (which measures the alignment of patterns in printing processes) compared to sheet-to-sheet (S2S) methods [1].

Over the past decades, models were developed to quantify the generation of machine direction or moving direction (MD) registration errors. Since registration error measures the misalignment between a given layer and those printed earlier, modeling and controlling these errors necessitate the consideration of time delays associated with the process. Models leveraging substrate strain variation and line moving speed to estimate MD registration errors were found in [2], [3], [4], [5]. Moreover, thermal effects on registration characteristics were incorporated in [6], and a data-driven algorithm to include unmodeled effects was given in [7].

Based on these models, control algorithms were developed to compensate for registration inaccuracies. Notably, nonlinear control schemes based on Lyapunov stability analysis were proposed in [3], [8] for single-span systems, and a decentralized control scheme was proposed in [9] for multi-span systems. Due to the interconnected nature of R2R printing systems, compensating for local process fluctuations can inadvertently introduce disturbances to other stages. Therefore, in [10], [11], controllers were designed to decouple the behavior of different printing sections. To counteract this coupling, an active disturbance rejection controller was proposed in [12], and a model predictive controller utilizing Padé approximation was given in [7].

It was shown that tension variations significantly contribute to registration errors in R2R processes [13]. Therefore, most aforementioned schemes aimed to address registration and tension fluctuations concurrently. However, the significance of safety as a prerequisite for control performance was often overlooked. In R2R printing sections, the ultimate objective is to minimize registration errors while limiting the tension to prevent failures like substrate breakage, thereby ensuring system safety. This refined focus enables the development of more effective and resilient registration control schemes in R2R processes.

Model predictive control (MPC) and reference governor (RG) are commonly used to handle constraints, but their applicability for registration control is limited. MPC struggles with controlling time delay systems due to the intense computational demands, while RG is limited to linear time delay systems [14]. Recently, safety functional-based methods emerged to address safety concerns in nonlinear time delay systems [15], [16], and control barrier functionals (CBFals) were developed to guide the design of safety control synthesis [17], [18]. Indeed, CBFal emerges as a preferable option for handling safety challenges in registration control.

This letter presents a comprehensive control framework for addressing the safety-critical aspects of registration accuracy

Manuscript received 15 September 2023; revised 12 November 2023; accepted 28 November 2023. Date of publication 5 December 2023; date of current version 22 December 2023. This work was supported by the Rackham Tuition Grant. Recommended by Senior Editor A. P. Aguiar. *(Corresponding author: Zhiyi Chen.)*

Zhiyi Chen is with the Department of Mechanical Engineering, University of Michigan at Ann Arbor, Ann Arbor, MI 48109 USA (e-mail: chzhiyi@umich.edu).

Gábor Orosz is with the Department of Mechanical Engineering and the Department of Civil and Environmental Engineering, University of Michigan at Ann Arbor, Ann Arbor, MI 48109 USA (e-mail: orosz@umich.edu).

Jun Ni is with the Department of Mechanical Engineering, University of Michigan at Ann Arbor, Ann Arbor, MI 48109 USA, and also with the Global Institute of Future Technology, Shanghai Jiao Tong University, Shanghai 200240, China (e-mail: junni@umich.edu).

Digital Object Identifier 10.1109/LCSYS.2023.3339446

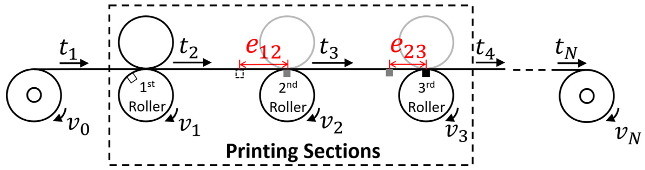

Fig. 1. An R2R system with three printing sections highlighted.

and tension control in R2R printing systems. The framework comprises a primary controller to reduce registration errors and maintain system stability under normal operating conditions. Additionally, a safety-critical controller is introduced, which interacts with the primary controller in a minimally-invasive fashion, ensuring the tension variations remain within specified limits. The main contribution of this letter is integrating safety-critical control into time-delayed R2R manufacturing systems, a concept that remains unexplored in the literature. Our numerical study is designed to motivate industry professionals to improve current industrial controllers with a straightforward yet effective method.

II. Modeling of Registration Errors

Fig. 1 illustrates an R2R printing system consisting of $(N-1)$ printing sections. Here, v_i represents the speed of the i^{th} roller (driven by a motor); t_i denotes the tension between the $(i-1)^{\text{th}}$ and i^{th} rollers; and $e_{i(i+1)}$ is the registration error between the i^{th} and $(i+1)^{\text{th}}$ printing rollers. It is assumed that no slippage occurs during the process, and all the printing rollers share the same radius. The objective is to ensure each layer is precisely stacked on top of its predecessor so that the registration error is minimized. This is achieved by adjusting roller speeds v_i.

Several mathematical models have been proposed to describe how the registration errors change in time [2], [3], [4], [5]. Here, we employ one specific model, which was validated experimentally in [3], [19], to demonstrate the effectiveness of the proposed method. The time evolution of the registration errors and tensions is given by

$$\begin{aligned}\dot{e}_{i(i+1)} &= \frac{AEv_{\mathrm{r}}}{AE+t_i(t-\tau_i)} - \frac{AEv_{\mathrm{r}}}{AE+t_{i+1}},\\ \dot{t}_{i+1} &= \frac{1}{L_{i+1}}\Big(t_iv_i - t_{i+1}v_{i+1} - AE\big(v_i - v_{i+1}\big)\Big),\end{aligned} \tag{1}$$

for $i=1,\dots,N-2$, where v_{r} is the reference speed of the printing system, A is the cross-section area of the substrate, E is Young's modulus, L_{i+1} is the span length of the substrate between i^{th} and $(i+1)^{\text{th}}$ rollers, and $\tau_i = L_{i+1}/v_{\mathrm{r}}$ is the time delay between the printing of two layers. The time argument t of the non-delayed terms is not spelled out for brevity.

For simplicity, two assumptions are made: i) the substrate tensions are well regulated by tension controllers at the entrance and exit of the printing sections, i.e., t_1 and t_N are constants; and ii) each section has the same length $L_i = L$ for $i=2,\dots,N-1$, resulting in the same time delay $\tau_i = \tau$ for $i=1,\dots,N-2$.

By defining the state vector and the input vector as

$$\begin{aligned}\boldsymbol{x} &= \big[e_{12}, e_{23}, \dots, e_{(N-2)(N-1)}, t_2, t_3, \dots, t_{N-1}\big]^\top \in \mathbb{R}^n,\\ \boldsymbol{u} &= \big[v_1, v_2, \dots, v_{N-1}\big]^\top \in \mathbb{R}^m,\end{aligned} \tag{2}$$

where $n = 2(N-2)$ and $m = N-1$, one can write (1) into the nonlinear, control affine form

$$\dot{\boldsymbol{x}}(t) = f(\boldsymbol{x}(t), \boldsymbol{x}(t-\tau)) + g(\boldsymbol{x}(t), \boldsymbol{x}(t-\tau))\boldsymbol{u}(t), \tag{3}$$

where $f:\mathbb{R}^n\times\mathbb{R}^n\to\mathbb{R}^n$ and $g:\mathbb{R}^n\times\mathbb{R}^n\to\mathbb{R}^{n\times m}$ are Lipschitz continuous functions. For example, considering three printing sections (cf. Fig. 1) we have $n=4$ and $m=3$.

III. Control Design

The overarching objective is to develop a registration controller that addresses two key aspects: i) mitigating registration errors, and ii) maintaining tension fluctuations within predefined limits to ensure system safety. To achieve these, the controller design is divided into two steps. Firstly, a primary controller is designed to stabilize the time delay system and eliminate registration errors during normal operation. Subsequently, a safety-critical controller is introduced, which intervenes in a minimally-invasive fashion when events that may jeopardize the safety of the system occur.

The following notations are used in the remaining sections.

1) $\mathcal{B}$ (Banach space) is the space of continuous functions mapping from $[-\tau, 0]$ to $\mathbb{R}^n$, which is equipped with the sup norm $\|\phi\| = \sup_{s\in[-\tau,0]}\|\phi(s)\|_2$, $\forall\phi\in\mathcal{B}$.
2) $\boldsymbol{x}_t : [-\tau, 0] \to \mathbb{R}^n$ represents the history of the state over $[t-\tau, t]$ with $\boldsymbol{x}_t(s) = \boldsymbol{x}(t+s)$, $s\in[-\tau,0]$.
3) $\boldsymbol{X}_t : [-\tau, 0] \to \mathbb{R}^n$ is the history of the linearized state over $[t-\tau, t]$ with $\boldsymbol{X}_t(s) = \boldsymbol{X}(t+s)$, $s\in[-\tau,0]$.

A. Primary Controller

In this section, a primary controller is designed based on the linear representation of R2R printing systems. Thus, we linearize (1) about the equilibrium $e_{i(i+1)}(t)\equiv 0$, $t_{i+1}(t)\equiv t_{\mathrm{r}}$, and $v_i(t)\equiv v_{\mathrm{r}}$ where t_{r} is the reference tension. Using the perturbations $E_{i(i+1)} = e_{i(i+1)}$, $T_i = t_i - t_{\mathrm{r}}$, and $V_i = v_i - v_{\mathrm{r}}$ we can define

$$\begin{aligned}\boldsymbol{X} &= \big[E_{12}, E_{23}, \dots, E_{(N-2)(N-1)}, T_2, T_3, \dots, T_{N-1}\big]^\top \in \mathbb{R}^n,\\ \boldsymbol{U} &= \big[V_1, V_2, \dots, V_{N-1}\big]^\top \in \mathbb{R}^m,\end{aligned} \tag{4}$$

where $n=2(N-2)$ and $m=N-1$, cf. (2). Then assuming $t_i \ll AE$, $i=1,\dots,N$, (3) yields the linear system

$$\dot{\boldsymbol{X}}(t) = A_0\boldsymbol{X}(t) + A_1\boldsymbol{X}(t-\tau) + B\boldsymbol{U}(t) \tag{5}$$

where $A_0\in\mathbb{R}^{n\times n}$, $A_1\in\mathbb{R}^{n\times n}$, and $B\in\mathbb{R}^{n\times m}$ are the system matrix, retarded system matrix, and input matrix, respectively.

For instance, consider a primary controller in the form $\boldsymbol{U}(t) = -K_{\mathrm{p}}\boldsymbol{X}(t)$, $K_{\mathrm{p}}\in\mathbb{R}^{m\times n}$. To establish the asymptotic stability (of the trivial solution) of (5), a quadratic Lyapunov-Krasovskii functional can be constructed:

$$V(\boldsymbol{X}_t) = \boldsymbol{X}^\top(t)P\boldsymbol{X}(t) + \int_{t-\tau}^{t}\boldsymbol{X}^\top(s)Q\boldsymbol{X}(s)\,\mathrm{d}s \tag{6}$$

where $P\in\mathbb{R}^{n\times n}$, $Q\in\mathbb{R}^{n\times n}$ are positive-definite matrices.

Definition 1 [20]: The system (5) is uniformly stable with the Lyapunov functional (6), if there exist K_{p} and a constant $\lambda > 0$, such that $V(\boldsymbol{X}_t)$ is positive definite and its derivative along (5) is non-positive for all $\boldsymbol{X}_t\in\mathcal{B}$, that is,

$$\frac{\mathrm{d}V}{\mathrm{d}t} = 2\boldsymbol{X}^\top(t)P\dot{\boldsymbol{X}}(t) + \boldsymbol{X}^\top(t)Q\boldsymbol{X}(t) - \boldsymbol{X}^\top(t-\tau)Q\boldsymbol{X}(t-\tau)$$

$$\begin{aligned}&= 2X^\top(t)P\big[(A_0 - BK_\text{p})X(t) + A_1X(t-\tau)\big]\\&\quad + X^\top(t)QX(t) - X^\top(t-\tau)QX(t-\tau)\\&\leq -\lambda|X(t)|^2,\end{aligned} \tag{7}$$

This leads to an equivalent linear matrix inequality [21]:

$$\begin{bmatrix}(A_0 - BK_\text{p})^\top P + P(A_0 - BK_\text{p}) + Q & PA_1\\ A_1^\top P & Q\end{bmatrix} < 0, \tag{8}$$

which implies that the choice of the control gain K_p needs to satisfy the following criteria to ensure stability:

1) $(A_0 - BK_\text{p})$ is Hurwitz, meaning every eigenvalue of the matrix has a negative real part.
2) $(A_0 - BK_\text{p}) \pm A_1$ is Hurwitz.
3) $(A_0 - BK_\text{p})^{-1}A_1$ is Schur, meaning all eigenvalues of the matrix have a magnitude less than one.

A similar conclusion was reached in [22], where matrix perturbation theory was used to design K_p. Here, we propose an algebraic Riccati equation (ARE) based method, which can be solved efficiently to compute a candidate control gain that satisfies the above criteria. This modified ARE approach can be applied to high-dimensional R2R systems.

Theorem 1: If there exist $Q > 0$ and $Q_1 > 0$, such that the modified ARE

$$A_0^\top P + PA_0 - PBB^\top P + PA_1Q^{-1}A_1^\top P + C^TC + Q + Q_1 = 0, \tag{9}$$

has a symmetric positive definite solution P, then the feedback control law

$$U(t) = -K_\text{p}X(t), \quad K_\text{p} = B^\top P, \tag{10}$$

stabilizes the time delay system (5) regardless of the time delay τ.

Proof: By the Schur complement theory, the linear matrix inequality (8) is equivalent to

$$\begin{aligned}&Q > 0,\\&(A_0 - BK_\text{p})^\top P + P(A_0 - BK_\text{p}) + Q + PA_1QA_1^\top P < 0.\end{aligned} \tag{11}$$

Substituting the control law (10) into (9), and subtracting $PBB^\top P$ from both sides, one can obtain

$$\begin{aligned}A_0^\top P + PA_0 - PBK_\text{p} + PA_1Q^{-1}A_1^\top P + Q - PBK_\text{p}&\\ = -C^\top C - Q_1 - PBB^\top P&\end{aligned} \tag{12}$$

Since $Q_1 > 0$ by definition, the right-hand side of (12) is negative, which implies the second inequality of (11). Thus, the proof is complete. ■

Considering that the controller (10) stabilizes the linearized system (5), the primary controller applied to the nonlinear system (3) becomes

$$u_\text{primary}(t) = u_\text{r} + U(t) = u_\text{r} - K_\text{p}(x(t) - x_\text{r}), \tag{13}$$

where $u_\text{r} = [v_\text{r}, v_\text{r}, \ldots, v_\text{r}]^\top$ is the reference control input that maintains the system at the steady state (the set point) $x_\text{r} = [0, 0, \ldots, 0, t_\text{r}, t_\text{r}, \ldots, t_\text{r}]^\top$. This control law is designed to stabilize an R2R printing system, but it does not explicitly consider the safety constraints.

B. Safety-Critical Controller Using CBFal

Unlike the previous section, where the primary controller is built upon a linearized model, here we design the safety-critical controller using the nonlinear control affine model (3). Particular attention is given to maintain tensions within a predefined limit, that is, to ensure that $t_i \in [t_\text{lb}, t_\text{ub}]$, to prevent excessive or insufficient tension. The following definition provides a mathematical characterization of safety in dynamical systems without time delays.

Definition 2 ([23, Def. 1] Safety of Delay-Free Systems): Consider a dynamic system described by ordinary differential equation $\dot{x}(t) = f(x(t))$, where $f : \mathbb{R}^n \to \mathbb{R}^n$ is a locally Lipschitz continuous function. The system is said to be safe w.r.t. set $S \subset \mathbb{R}^n$, if S is forward invariant, i.e., $x(0) \in S \Rightarrow x(t) \in S$, $\forall t \geq 0$.

Definition 2 states that a delay-free system is considered safe if the initial state $x(0)$ belonging to the safe set S guarantees that the subsequent evolution of the system remains within S. This definition of safety can be extended to autonomous time delay systems of the form

$$\dot{x}(t) = \mathcal{F}(x_t), \tag{14}$$

where $\mathcal{F} : \mathcal{B} \to \mathbb{R}^n$ is a locally Lipschitz continuous functional [24], [25], [26]. This system has a unique solution, given any state history $x_0 \in \mathcal{B}$. Following Definition 2, the safety of system (14) can be defined as follows.

Definition 3 ([17, Def. 5] Safety of Time Delay Systems): System (14) is said to be safe w.r.t set $\mathcal{S} \subset \mathcal{B}$, if $\mathcal{S}$ is forward invariant s.t. $x_0 \in \mathcal{S} \Rightarrow x_t \in \mathcal{S}$, $\forall t \geq 0$.

The following theorem addresses the construction of the forward invariant set $\mathcal{S}$ and the so-called barrier functional (also called safety functional).

Theorem 2 [15, Th. 2]: Given that the set $\mathcal{S}$ is a 0-superlevel set of a continuously differentiable functional $\mathcal{H}$ satisfying

$$\mathcal{S} = \{x_t \in \mathcal{B} : \mathcal{H}(x_t) \geq 0\}, \tag{15}$$

then $\mathcal{H}$ is a safety functional if it satisfies

$$\dot{\mathcal{H}}(x_t, \dot{x}_t) \geq -\alpha(\mathcal{H}(x_t)), \tag{16}$$

where $\alpha : [0, a] \to [0, \infty]$ is a class $\mathcal{K}$ function. Note that $\dot{\mathcal{H}}(\cdot)$ is the time derivative of $\mathcal{H}$ along (14).

We now introduce the concept of control barrier functional (CBFal) that will enable us to synthesize safety-critical controllers. By considering the control input, (14) can be extended to the form

$$\dot{x}(t) = \mathcal{F}(x_t) + \mathcal{G}(x_t)u(t), \tag{17}$$

where $\mathcal{F} : \mathcal{B} \to \mathbb{R}^n$ and $\mathcal{G} : \mathcal{B} \to \mathbb{R}^{n\times m}$ are locally Lipschitz continuous functionals. Note that the nonlinear model (3) can be written in the form of (17). Our goal is to design a controller that keeps the system within the safe set $\mathcal{S}$. To achieve this, we require the following.

Definition 4 [17, Def. 7]: Given the forward invariant set $\mathcal{S}$ defined by (15), a continuously differentiable functional $\mathcal{H}$ is a CBFal for system (17) if it satisfies

$$\sup_{u\in\mathbb{R}^m} \dot{\mathcal{H}}(x_t, \dot{x}_t, u) \geq -\alpha(\mathcal{H}(x_t)), \tag{18}$$

where $\alpha : [0, a] \to [0, \infty]$ is a class $\mathcal{K}$ function. Here $\dot{\mathcal{H}}(\cdot)$ denotes the time derivative of $\mathcal{H}$ which can be calculated as

$$\dot{\mathcal{H}}(\boldsymbol{x}_t, \dot{\boldsymbol{x}}_t, \boldsymbol{u}) = \mathcal{L}_{\mathcal{F}}\mathcal{H}(\boldsymbol{x}_t, \dot{\boldsymbol{x}}_t) + \mathcal{L}_{\mathcal{G}}\mathcal{H}(\boldsymbol{x}_t)\boldsymbol{u}, \tag{19}$$

with functionals $\mathcal{L}_{\mathcal{F}}\mathcal{H} : \mathcal{B} \to \mathbb{R}$ and $\mathcal{L}_{\mathcal{G}}\mathcal{H} : \mathcal{B} \to \mathbb{R}^{1\times m}$.

For simplicity, we introduce a short hand notation where x_i represents the i^{th} element of $\boldsymbol{x}(t) = \boldsymbol{x}_t(0)$. Then, we define the CBFal candidate

$$\mathcal{H}(\boldsymbol{x}_t) = 1 - \sqrt[p]{\sum_{i=1}^{n} w_i \left(\frac{x_i - a_i}{b_i}\right)^p}, \tag{20}$$

where p is an even number, w_i are the i^{th} element of a weight vector $\boldsymbol{w}$, while a_i and b_i are the i^{th} elements of

$$\mathbf{a} = \frac{\boldsymbol{x}_{\max} + \boldsymbol{x}_{\min}}{2}, \quad \boldsymbol{b} = \frac{\boldsymbol{x}_{\max} - \boldsymbol{x}_{\min}}{2}, \tag{21}$$

respectively. The high-order norms in (20) are used to fill the domain between the upper and lower bounds given by $\boldsymbol{x}_{\min} \in \mathbb{R}^n$ and $\boldsymbol{x}_{\max} \in \mathbb{R}^n$, while maintaining the smoothness of the CBFal. Since (20) does not depend on the delayed states, the $\dot{\boldsymbol{x}}_t$ term vanishes in $\dot{\mathcal{H}}(\cdot)$; cf. (18) and (19).

If the inequality (18) is satisfied for $\boldsymbol{u}_{\text{primary}}$ (cf. (13)), then the primary controller is capable of keeping the system states within the safe set. Otherwise, adjustments must be made to the primary controller to maintain safety. To achieve this, a minimally invasive controller can be constructed by using the following quadratic programming optimization problem

$$\begin{aligned} &\min_{\boldsymbol{u}\in\mathbb{R}^m} \ \|\boldsymbol{u} - \boldsymbol{u}_{\text{primary}}\|_2^2 \\ &\text{subject to } \ \dot{\mathcal{H}}(\boldsymbol{x}_t, \boldsymbol{u}) \geq -\alpha(\mathcal{H}(\boldsymbol{x}_t)). \end{aligned} \tag{22}$$

An explicit solution to this optimization problem can be obtained by Karush-Kuhn-Tucker conditions [17]:

$$\boldsymbol{u} = \begin{cases} \boldsymbol{u}_{\text{primary}} & \text{if } \phi(\boldsymbol{x}_t) \geq 0, \\ \boldsymbol{u}_{\text{primary}} - \dfrac{\phi(\boldsymbol{x}_t)\phi_0^\top(\boldsymbol{x}_t)}{\phi_0(\boldsymbol{x}_t)\phi_0^\top(\boldsymbol{x}_t)} & \text{otherwise,} \end{cases} \tag{23}$$

where

$$\begin{aligned} \phi_0(\boldsymbol{x}_t) &= \mathcal{L}_{\mathcal{G}}\mathcal{H}(\boldsymbol{x}_t), \\ \phi(\boldsymbol{x}_t) &= \mathcal{L}_{\mathcal{F}}\mathcal{H}(\boldsymbol{x}_t) + \mathcal{L}_{\mathcal{G}}\mathcal{H}(\boldsymbol{x}_t)\boldsymbol{u}_{\text{primary}} + \alpha(\mathcal{H}(\boldsymbol{x}_t)). \end{aligned} \tag{24}$$

Note that the existence of such a closed-form analytic solution is based on the assumption that the admissible range of control inputs is sufficiently large, i.e., that $\boldsymbol{u}$ can be as large as needed. This holds for the R2R application, where the torques available to control the roller speed are much larger than those applied at the substrates. The controller provides the following guarantee:

Proposition 1: Consider a nonlinear control affine system defined in (3). Let the safety-critical controller be synthesized according to (13) and (23). It provides:

1) Local asymptotic stability of the set point when the system states are within the interior of the safe set.
2) Forward invariance of the safe set, thereby ensuring safety by preventing the states from leaving the set.

Furthermore, the resulting controller is Lipschitz continuous, resulting in seamless transitions between the primary controller and the safety controller.

TABLE I
SYSTEM PARAMETERS USED FOR SIMULATIONS

Symbol	Parameter	Value
A	Cross-sectiona area	1.2×10^{-5} (m^2)
E	Young's modulus	200 (MPa)
L	Span length	0.2 (m)
v_{r}	Speed reference	0.01 (m/s)
t_{r}	Tension reference	30 (N)
t_{lb}	Tension lower bound	29 (N)
t_{ub}	Tension upper bound	31 (N)

Note that even though in our case (23) employs (13) as the primary controller, users can substitute it with the original registration controllers installed in their systems. This highlights the practical significance of the safety-critical control scheme presented here, as it can be readily implemented on existing production systems without the need for complex modifications to the overall control logic.

IV. CASE STUDY

A simulation study is conducted to evaluate the performance of the proposed controller in an R2R system with three printing rollers; see Fig. 1. The state and input vectors (2) become $\boldsymbol{x} = [e_{12},\ e_{23},\ t_2,\ t_3]^\top$, $\boldsymbol{u} = [v_1,\ v_2,\ v_3]^\top$ while the nonlinear function in (3) become

$$f = \left[\tfrac{AEv_{\text{r}}}{AE+t_1(t-\tau)} - \tfrac{AEv_{\text{r}}}{AE+t_2},\ \tfrac{AEv_{\text{r}}}{AE+t_2(t-\tau)} - \tfrac{AEv_{\text{r}}}{AE+t_3},\ 0,\ 0\right]^\top,$$
$$g = \begin{bmatrix} 0 & 0 & 0 \\ 0 & 0 & 0 \\ \frac{1}{L}(t_1 - AE) & \frac{1}{L}(AE - t_2) & 0 \\ 0 & \frac{1}{L}(t_2 - AE) & \frac{1}{L}(AE - t_3) \end{bmatrix}. \tag{25}$$

The parameters are presented in Table I. These are identified from a single-stage R2R printing system and then expanded to a multistage R2R to demonstrate the scalability of the proposed method; see [27] for more information.

The system dynamics are simulated using the nonlinear model (1), which is solved using the dde23 in MATLAB. The simulation duration is set to 80 s, and a sampling time of 10 ms is chosen. We first simulate the case where only the primary controller is deployed to the system, then implement the safety-critical controller.

A. Implementation Details

We assume that the R2R printing system is initially operating at a steady state. At $t = 10$ s, the registration error $e_{12} = 100$ μm is applied between the first and second printing units. To compensate for the registration error, a primary controller is designed according to the modified ARE (9) and the control law (10). The corresponding control gain matrix is determined to be

$$K_{\text{p}} = \begin{bmatrix} 79.6311 & 57.0547 & -0.0025 & -0.0007 \\ -55.4414 & 189.5500 & 0.0018 & -0.0018 \\ -24.1897 & -246.6074 & 0.0007 & 0.0025 \end{bmatrix}.$$

Then, the CBFal (20) is constructed. Typically, no constraints are considered for the registration errors, but $\pm5\%$ tension margin is allowed in high-precision R2R processes.

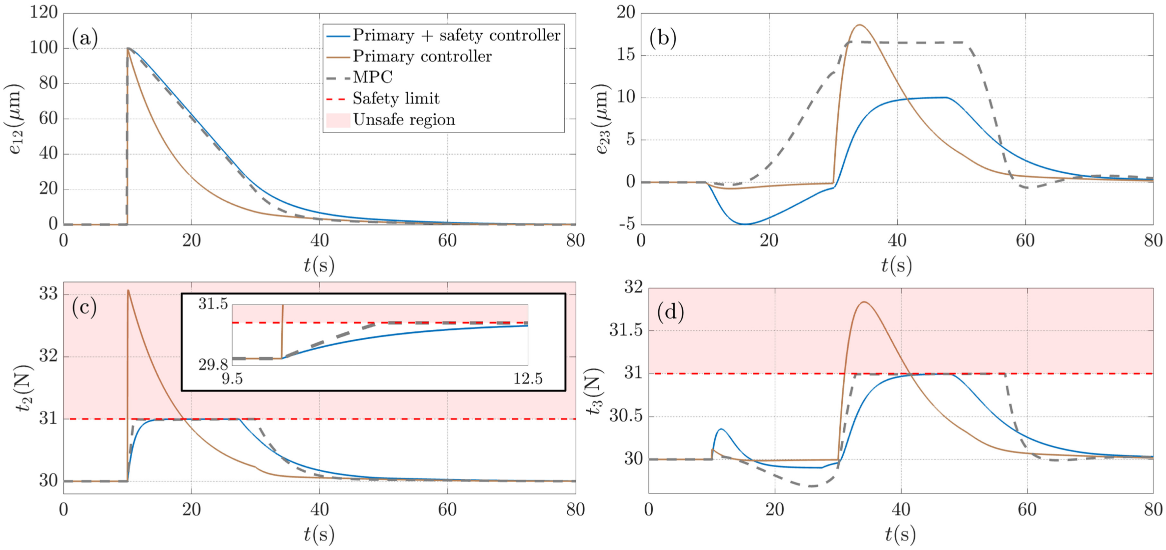

Fig. 2. Registration error responses (a) e_{12} and (b) e_{23}, and tension responses (c) t_2 and (d) t_3 when an initial registration error in e_{12} occurs at $t = 10$ s. Registration errors are eliminated in both cases, while the safety-critical controller keeps the tension variations within the safe domain.

In our case, this means ±1 N from the nominal value 30 N. Therefore, the weight vector and the control limits are

$$\boldsymbol{w} = \begin{bmatrix} 0 \\ 0 \\ 1 \\ 1 \end{bmatrix}, \quad \boldsymbol{a} = \begin{bmatrix} \cdot \\ \cdot \\ 30 \\ 30 \end{bmatrix}, \quad \boldsymbol{b} = \begin{bmatrix} \cdot \\ \cdot \\ 1 \\ 1 \end{bmatrix}, \tag{26}$$

cf. (21) while (20) becomes

$$\mathcal{H}(\boldsymbol{x}_t) = 1 - \sqrt[4]{\left(\frac{x_3 - a_3}{b_3}\right)^4 + \left(\frac{x_4 - a_4}{b_4}\right)^4}. \tag{27}$$

The time derivative of $\mathcal{H}$ along (3), which appears in (18), becomes

$$\dot{\mathcal{H}}(\boldsymbol{x}_t) = \underbrace{\left[0\ 0\ h_3\ h_4\right] f(\boldsymbol{x}(t), \boldsymbol{x}(t-\tau))}_{\mathcal{L}_{\mathcal{F}}\mathcal{H}(\boldsymbol{x}_t)}, + \underbrace{\left[0\ 0\ h_3\ h_4\right] g(\boldsymbol{x}(t), \boldsymbol{x}(t-\tau))}_{\mathcal{L}_{\mathcal{G}}\mathcal{H}(\boldsymbol{x}_t)} \boldsymbol{u}(t), \tag{28}$$

where

$$h_i = \frac{\partial \mathcal{H}}{\partial x_i} = -w_i \left(\frac{x_i - a_i}{b_i}\right)^{p-1} \left(\sum_{i=1}^{n} w_i \left(\frac{x_i - a_i}{b_i}\right)^p\right)^{\frac{1-p}{p}}$$
$$= -\left(\frac{x_i - a_i}{b_i}\right)^3 \left(\left(\frac{x_3 - a_3}{b_3}\right)^4 + \left(\frac{x_4 - a_4}{b_4}\right)^4\right)^{-\frac{3}{4}}, \tag{29}$$

for $i = 3, 4$. Moreover, (13) and (24) result in

$$\phi_0(\boldsymbol{x}_t) = \left[0\ 0\ h_3\ h_4\right] g(\boldsymbol{x}(t), \boldsymbol{x}(t-\tau)),$$
$$\phi(\boldsymbol{x}_t) = \left[0\ 0\ h_3\ h_4\right] f(\boldsymbol{x}(t), \boldsymbol{x}(t-\tau)) + \left[0\ 0\ h_3\ h_4\right] g(\boldsymbol{x}(t), \boldsymbol{x}(t-\tau)) \left(\boldsymbol{u}_{\mathrm{r}} - K_{\mathrm{p}}(\boldsymbol{x}(t) - \boldsymbol{x}_{\mathrm{r}})\right) + 1 - \sqrt[4]{\left(\frac{x_3 - a_3}{b_3}\right)^4 + \left(\frac{x_4 - a_4}{b_4}\right)^4}, \tag{30}$$

where $\alpha(r) = r$ was the chosen class $\mathcal{K}$ function. To verify (20) is a valid CBFal, one can show numerically that $\phi_0(\boldsymbol{x}_t) \neq 0$ within the safe set, by using (25), (28) and (29).

Note that the candidate function in (20) involves only delay-free terms, as the delayed states do not pertain to the safety considerations in this case. A general form of the Lie derivatives $\mathcal{L}_{\mathcal{F}}\mathcal{H}$ and $\mathcal{L}_{\mathcal{G}}\mathcal{H}$ for systems involving multiple or distributed delays can be found in [17].

B. Control Performance

The simulation results are presented in Fig. 2. The brown curves in Fig. 2(a) show that the primary controller effectively eliminates the introduced registration error e_{12} within about 40 s. During this period, a nonzero registration error e_{23} is also observed at the downstream printing unit, as shown in Fig. 2(b), resulting from the control actions taken to compensate for the upstream errors. The primary controller also eliminated this error. In addition, the actions of the primary controller cause tension variations, as shown in Fig. 2(c)–(d). Since the induced tension variations exceed 1 N, they pose a safety risk.

The blue curves in Fig. 2 represent the responses when the safety-critical controller is introduced. In this case, the registration errors are reduced in a less aggressive manner, resulting in a slower rate of decrease. In the meantime, the tension variations are constrained within the specified limits. The safety-critical controller ensures the safe operation of the system without altering the stability properties. An unintended benefit can also be observed in Fig. 2(b), where the tension constraints help reduce the peak magnitude of e_{23}.

The dashed curves in Fig. 2 represent the responses from a classic constrained MPC generated using the MATLAB MPC designer toolbox. Compared to MPC, our approach has three benefits: i) the explicit solution in (23) reduces computation time (around tenfold); ii) the enforcement of the safety constraints is manifested by a gradual, smooth approach toward the safe boundary; and iii) the proposed safety-critical control synthesis can be combined with any existing controller from [9], [10], [11], [12] to enhance their performance in safety-critical environments. To understand this, we have also implemented a primary controller using the pole placement

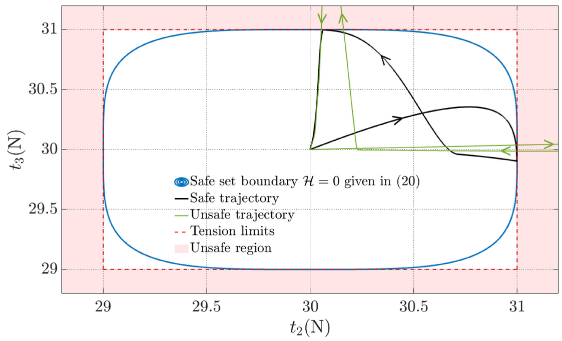

Fig. 3. Required tension limits (dashed red lines), safe set boundary (20) (blue curve), and system responses when applying the primary controller only (green trajectory) and adding with safety control (black trajectory).

design from [22]. Our proposed control synthesis still enforced the tension limits, but the overall control performance fell short of expectations due to the choice of the primary controller.

Fig. 3 shows the safety region defined by the CBFal (27). The green trajectory shows the response of the system when applying the primary controller. After the initial perturbations are applied, the system returns to the equilibrium, but in the meantime, it leaves the safe set and enters the unsafe region of the state space. Applying the safety-critical controller, as shown by the black trajectory, the tension responses are constrained by the boundaries of the safe set, preventing system failures caused by excessive tension variations.

V. Conclusion

In this letter, we addressed a control problem in R2R printing, focusing on improving registration accuracy and system safety. We proposed a control framework that combines a primary controller and a safety controller. To obtain the primary controller, a modified ARE was designed based on the linearized delay model. Then, a control barrier functional is constructed to ensure the system safety. In the numerical study, we observed that the primary controller successfully eliminated registration errors, while the safety controller constrained the tension variations within prescribed limits. The proposed approach can be readily implemented in practical systems without the need for online computation, making it suitable for real-time control applications.

One limitation of the proposed algorithm is the requirement for an accurate registration model, which can be difficult to obtain due to the complex behavior of R2R printing systems. Also, the work only considered cases where time delays are identical among stages, but the framework established can be extended to the case of multiple delays. Future research can explore experimental validation of the proposed control approach in industrial-scale R2R printing systems. Also, the robustness of the approach can be improved by considering model uncertainties and external disturbances.

References

[1] J. Willmann, D. Stocker, and E. Dörsam, "Characteristics and evaluation criteria of substrate-based manufacturing. is roll-to-roll the best solution for printed electronics?" *Organic Electron.*, vol. 15, no. 7, pp. 1631–1640, 2014.

[2] A. Seshadri, P. R. Pagilla, and J. E. Lynch, "Modeling print registration in roll-to-roll printing presses," *J. Dyn. Sys., Meas., Control*, vol. 135, no. 3, 2013, Art. no. 031016.

[3] T. Yoshida, S. Takagi, Y. Muto, and T. Shen, "Register control of rotogravure printing press. application of nonlinear control theory to sectional drive printing press," *Electron. Commun. Jpn.*, vol. 94, no. 1, pp. 17–24, 2011.

[4] S. Liu, X. Mei, J. Li, and L. Ma, "Machine directional register system modeling for shaft-less drive gravure printing machines," *Math. Problems Eng.*, vol. 2013, Nov. 2013, Art. no. 251636.

[5] H. Kang, C. Lee, and K. Shin, "Modeling and compensation of the machine directional register in roll-to-roll printing," *Control Eng. Pract.*, vol. 21, no. 5, pp. 645–654, 2013.

[6] J. Lee, K. Shin, and C. Lee, "Analysis of dynamic thermal characteristic of register of roll-to-roll multi-layer printing systems," *Robot. Comput.-Integr. Manuf.*, vol. 35, pp. 77–83, Oct. 2015.

[7] K. Shah, A. He, Z. Wang, X. Du, and X. Jin, "Data-driven model predictive control for roll-to-roll process register error," in *Proc. Int. Manuf. Sci. Eng. Conf.*, 2022, Art. no. V001T03A006.

[8] K. H. Choi et al., "Web register control algorithm for roll-to-roll system based printed electronics," in *Proc. IEEE Int. Conf. Autom. Sci. Eng.*, 2010, pp. 867–872.

[9] A. Seshadri and P. R. Pagilla, "Decentralized control of print registration in roll-to-roll printing presses," in *Proc. Dyn. Syst. Control Conf.*, 2013, Art. no. V001T14A006.

[10] T. Zhang, Z. He, and Z. Chen, "A decoupling matrix-based learning control scheme for the machine directional register of roll-to-roll systems," *IEEE Trans. Ind. Electron.*, vol. 70, no. 8, pp. 8398–8407, Aug. 2023.

[11] Z. Chen, T. Zhang, Y. Zheng, D. S.-H. Wong, and Z. Deng, "Fully decoupled control of the machine directional register in roll-to-roll printing system," *IEEE Trans. Ind. Electron.*, vol. 68, no. 10, pp. 10007–10018, Oct. 2021.

[12] S. Liu, B. Yin, L. Ma, H. Xu, and G. Zhu, "A decoupling control strategy for multilayer register system in printed electronic equipment," *Math. Problems Eng.*, vol. 2016, Sep. 2016, Art. no. 7165163.

[13] A. N. Gafurov et al., "Registration error analysis and compensation of roll-to-roll screen printing system for flexible electronics," *Flex. Print. Electron.*, vol. 6, no. 2, 2021, Art. no. 024003.

[14] N. Li, S. Geng, I. Kolmanovsky, and A. Girard, "An explicit reference governor for linear sampled-data systems with disturbance inputs and uncertain time delays," *IEEE Trans. Autom. Control*, vol. 68, no. 1, pp. 440–447, Jan. 2023.

[15] G. Orosz and A. D. Ames, "Safety functionals for time delay systems," in *Proc. Am. Control Conf. (ACC)*, 2019, pp. 4374–4379.

[16] A. K. Kiss, T. G. Molnár, D. Bachrathy, A. D. Ames, and G. Orosz, "Certifying safety for nonlinear time delay systems via safety functionals: A discretization based approach," in *Proc. Amer. Control Conf. (ACC)*, 2021, pp. 1058–1063.

[17] A. K. Kiss, T. G. Molnár, A. D. Ames, and G. Orosz, "Control barrier functionals: Safety-critical control for time delay systems," *Int. J. Robust Nonlin. Control*, vol. 33, no. 12, pp. 7282–7309, 2023.

[18] W. Liu, Y. Bai, L. Jiao, and N. Zhan, "Safety guarantee for time-delay systems with disturbances," *Sci. China Inf. Sci.*, vol. 66, pp. 132102:1–132102:15, 2021. [Online]. Available: http://doi.org/10.1007/s11432-020-3266-6

[19] Z. Chen, Y. Zheng, T. Zhang, D. S.-H. Wong, and Z. Deng, "Modeling and register control of the speed-up phase in roll-to-roll printing systems," *IEEE Trans. Autom. Sci. Eng.*, vol. 16, no. 3, pp. 1438–1449, Jul. 2019.

[20] K. Gu, V. L. Kharitonov, and J. Chen, *Stability of Time-Delay System*. Boston, MA, USA: Birkhäuser, 2003. [Online]. Available: https://link.springer.com/book/10.1007/978-1-4612-0039-0#bibliographic-information

[21] E. Fridman, "Tutorial on Lyapunov-based methods for time-delay systems," *Eur. J. Control*, vol. 20, no. 6, pp. 271–283, 2014.

[22] A. Seshadri and P. R. Pagilla, "Design of delay independent state feedback control for roll-to-roll printing applications," in *Proc. Dyn. Syst. Control Conf.*, 2014, Art. no. V003T28A004.

[23] A. D. Ames, S. Coogan, M. Egerstedt, G. Notomista, K. Sreenath, and P. Tabuada, "Control barrier functions: Theory and applications," in *Proc. 18th Eur. Control Conf. (ECC)*, 2019, pp. 3420–3431.

[24] G. Stépán, *Retarded Dynamical Systems*. Harlow, U.K.: Longman, 1989.

[25] O. Diekmann, S. A. van Gils, S. M. Verduyn Lunel, and H.-O. Walther, *Delay Equations*. New York, NY, USA: Springer, 1995. [Online]. Available: https://link.springer.com/book/10.1007/978-1-4612-4206-2#bibliographic-information

[26] D. Breda, S. Maset, and R. Vermiglio, *Stability of Linear Delay Differential Equations*. New York, NY, USA: Springer, 2015.

[27] Z. Chen, B. Qu, B. Jiang, S. R. Forrest, and J. Ni, "Robust constrained tension control for high-precision roll-to-roll processes," *ISA Trans.*, vol. 136, pp. 651–662, May 2023.